GEOPHYSICAL RESEARCH LETTERS, VOL. 34, L03818, doi:10.1029/2006GL028149, 2007

On the sensitivity of radiative forcing from biomass burning aerosols and ozone to emission location

Vaishali Naik,[1] Denise L. Mauzerall,[1,2] Larry W. Horowitz,[3] M. Daniel Schwarzkopf,[3] V. Ramaswamy,[3] and Michael Oppenheimer[1,2]

Received 13 September 2006; revised 27 December 2006; accepted 27 December 2006; published 13 February 2007.

[1] Biomass burning is a major source of air pollutants, some of which are also climate forcing agents. We investigate the sensitivity of direct radiative forcing due to tropospheric ozone and aerosols (carbonaceous and sulfate) to a marginal reduction in their (or their precursor) emissions from major biomass burning regions. We find that the largest negative global forcing is for 10% emission reductions in tropical regions, including Africa (-4.1 mWm^{-2} from gas and -4.1 mWm^{-2} from aerosols), and South America (-3.0 mWm^{-2} from gas and -2.8 mWm^{-2} from aerosols). We estimate that a unit reduction in the amount of biomass burned in India produces the largest negative ozone and aerosol forcing. Our analysis indicates that reducing biomass burning emissions causes negative global radiative forcing due to ozone and aerosols; however, regional differences need to be considered when evaluating controls on biomass burning to mitigate global climate change. **Citation:** Naik, V., D. L. Mauzerall, L. W. Horowitz, M. D. Schwarzkopf, V. Ramaswamy, and M. Oppenheimer (2007), On the sensitivity of radiative forcing from biomass burning aerosols and ozone to emission location, *Geophys. Res. Lett.*, *34*, L03818, doi:10.1029/2006GL028149.

1. Introduction

[2] Approximately 90% of biomass burning (BB), including burning of forests, grasslands, and agricultural waste for land clearing and land use change, is ascribed to anthropogenic activities [*Andreae*, 1991]. Increases or decreases in anthropogenic BB in the future will likely depend on the whether control measures are implemented [*Streets et al.*, 2004]. Future levels of control on BB remain difficult to predict and will likely vary by region. BB is a significant source of tropospheric ozone (O_3) precursors including nitrogen oxides (NO_x), carbon monoxide (CO) and non-methane volatile organic compounds (NMVOCs); aerosol precursors such as sulfur dioxide (SO_2); and primary aerosols including organic carbon (OC) and black carbon (BC). Numerous measurement and modeling studies have demonstrated the influence of BB emissions on tropospheric O_3 [*Kim and Newchurch*, 1996; *Mauzerall et al.*, 1998; *Thompson et al.*, 2001; *McKeen et al.*, 2002], and on the radiative balance of the Earth [*Ramaswamy et al.*, 2001]. The global radiative forcing (RF) due to changes in tropospheric O_3 (from all sources) since preindustrial time is estimated to be $+0.35$ Wm^{-2} (at the tropopause with an uncertainty of ±43%), while the direct RF due to BB aerosols at the top of the atmosphere ranges from -0.07 to -0.6 Wm^{-2} with a mean estimate of -0.2 Wm^{-2} [*Ramaswamy et al.*, 2001, and references therein]. This estimate for RF due to BB aerosols does not include the indirect RF resulting from aerosol-induced changes in cloud properties.

[3] Reducing BB emissions has been estimated to cause a short term warming (by reducing reflective aerosols), but a long term cooling from reducing CO_2 (particularly by avoiding permanent deforestation) and other greenhouse gases, and has been proposed as a control strategy for mitigating climate change [*Jacobson*, 2004]. Thorough investigation of the climate forcing response to changes in BB emissions is therefore needed to inform climate change policy. World regions are characterized by different types of vegetation fires (forests, savannas, and agricultural waste) that differ not only in the amount of biomass burned but also in the mixture of trace species emitted. Regional differences in BB will, therefore, have implications for global radiative forcing on climate. However, the sensitivity of trace gas and aerosol radiative forcing to the geographical location of BB has not previously been analyzed.

[4] Here we build upon our previous study [*Naik et al.*, 2005] to assess the global RF from reductions in regional BB emissions of short-lived tropospheric O_3 precursors and aerosols. Using a global chemical transport model, we simulate the changes in the distributions of tropospheric O_3 and aerosols in response to a sustained marginal reduction (10%) in BB emissions from each of seven major biomass burning regions: Africa, East Asia, the Former Soviet Union, India, North America, South America, and Southeast Asia. We then examine the global RF resulting from the perturbations to O_3 and aerosol concentrations. We focus on the effect of marginal reductions in BB emissions in order to approximate the impact of potentially feasible reductions in BB emissions.

2. Methods

[5] We perform base case and perturbation simulations using the Model for OZone And Related Tracers version 2 (MOZART-2) [*Horowitz et al.*, 2003] which includes the chemistry and transport of gaseous and aerosol species [*Tie et al.*, 2005]. In this study, MOZART-2 simulations are performed at a horizontal resolution of 2.8° latitude × 2.8° longitude with 34 hybrid vertical levels forced by meteoro-

[1]Woodrow Wilson School of Public and International Affairs, Princeton University, Princeton, New Jersey, USA.
[2]Also at Department of Geosciences, Princeton University, Princeton, New Jersey, USA.
[3]Geophysical Fluid Dynamics Laboratory, NOAA, Princeton, New Jersey, USA.

0094-8276/07/2006GL028149$05.00

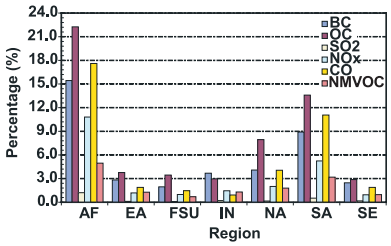

Figure 1. Percentage that regional biomass burning contributes to global total emissions of O_3 precursors and aerosol species.

logical variables from the middle atmosphere version of the NCAR Community Climate Model (MACCM3) [*Kiehl et al.*, 1998]. All simulations are run for 25 months and results from the final 12 months are analyzed.

[6] Surface emissions of all chemical species in the base simulation are prescribed from the MOZART-2 emission inventory used by *Horowitz et al.* [2003] that is representative of the early 1990s. In particular, BB emissions from forests, savanna and agricultural waste (excluding agricultural waste used as biofuel) burning are calculated from the emission ratios of *Andreae and Merlet* [2001] and biomass burned from *Müller* [1992] and *Hao and Liu* [1994] (see auxiliary material).[1] The largest BB emissions of O_3 precursors, BC, OC, and SO_2 (precursor to $SO_4^=$) come from Africa followed by South America (Figure 1). Globally, BB emissions of OC are approximately 6 times larger by mass than those of BC and 8 times larger than SO_2 (precursor to sulfate) (see auxiliary material Table S2), however, the OC/BC emission ratio varies by region depending on the dominant type of vegetation burning. The OC/BC ratio is highest for boreal and temperate forest burning ($\sim$16) followed by tropical forests ($\sim$8) and savanna burning ($\sim$7), and smallest for agricultural waste burning ($\sim$3) [*Andreae and Merlet*, 2001]. The wide range in emission ratios is ascribed to the differences in fuel composition and combustion types. While for most regions the percentage of OC emissions is higher than BC emissions relative to the global total emissions, in India, the BC emissions percentage is higher than OC emissions percentage due to the dominance of agricultural waste burning (Figure 1) [*Streets et al.*, 2003].

[7] Our base simulation produces a global annual average tropospheric O_3 column of 30.1 DU (calculated up to the "chemical tropopause" of 150 ppbv O_3), and a column burden of 2.5 mg/m^2 of OC, 0.5 mg/m^2 of BC and 5.0 mg/m^2 of $SO_4^=$. Our simulated ozone and aerosol distributions are similar to those obtained from previous simulations of MOZART-2 that have been extensively evaluated against measurements [*Horowitz et al.*, 2003; *Ginoux et al.*, 2006]. The modeled tropospheric O_3 concentrations agree reasonably well with observations [*Horowitz et al.*, 2003] and the simulated annual mean aerosol concentrations generally match the observations to within a factor of two, but tend to be overestimated in polluted regions [*Ginoux et al.*, 2006]. Significant differences in our simulated vertical aerosol distributions compared with that of previous modeling studies are likely due to the different treatments of vertical mixing and aerosol emissions and wet deposition [*Ginoux et al.*, 2006]. Vertical aerosol profiles, relevant for aerosol RF calculations, have been shown to vary considerably across models [*Textor et al.*, 2006] and need to be evaluated against measurements as high temporally and spatially resolved data become available in the future.

[8] Following the methodology of *Naik et al.* [2005], we perform perturbation simulations in which surface BB emissions of NO_x, CO, NMVOCs, BC, OC, and SO_2 from each region are reduced by 10%, maintaining the spatial and temporal distribution of emissions. Although methane (CH_4) is emitted from BB, we do not reduce its emissions as we focus on short-lived species here. We allow CH_4 concentrations to respond to emissions and losses in all simulations, but the concentrations do not reach a new steady state within the timescale of our model runs. The long-lived "primary mode" perturbation to CH_4 concentrations causes a delayed response in O_3 concentration in addition to the initial rapid O_3 reduction [*Wild et al.*, 2001]. We estimate the steady-state primary mode changes in global CH_4 and O_3 concentrations and the resulting RF following [*Naik et al.*, 2005].

[9] We use the offline Geophysical Fluid Dynamic Laboratory (GFDL) radiative transfer model (RTM) [*GFDL Global Atmospheric Model Development Team*, 2004; *Naik et al.*, 2005; *Ming et al.*, 2005] to perform RF calculations. We simulate the monthly mean net radiation fluxes for the base and perturbed O_3 and aerosol distributions and then calculate RF as the difference in the net fluxes from the two simulations [*Naik et al.*, 2005]. We calculate RF due to aerosol perturbations at the top-of-the-atmosphere (TOA), while RF due to O_3 perturbations is computed at the tropopause after allowing for stratospheric temperatures to adjust to equilibrium. "Stratospheric adjustment" causes RF at the tropopause to be equivalent to TOA RF, which is a good indicator of the resulting changes in global mean surface temperature [*Committee on Radiative Forcing Effects on Climate*, 2005]. The radiative properties of aerosol components in the model are described by *Ginoux et al.* [2006] (an error in the specific extinction coefficient of OC noted by *Ginoux et al.* [2006] was corrected in this version of the model). We estimate the aerosol direct RF assuming external mixtures thus providing a lower limit for the RF from BC. An internal mixture of BC and $SO_4^=$ or OC and $SO_4^=$ has been suggested to be more absorbing, resulting in a more positive forcing than from a corresponding external mixture [*Haywood and Boucher*, 2000]. In this study, we do not consider the influence of BB aerosols on cloud properties, which has been estimated to produce a strong negative forcing from reduction in cloud droplet size and reflectance [*Ramaswamy et al.*, 2001, and references therein]. Hygroscopic growth of OC is not considered in this version of the model which may cause us to underestimate its forcing by 18–32% [*Ming et al.*, 2005]. We compute CH_4 RF resulting from the primary mode perturbation using the formulation of *Intergovernmental Panel on Climate Change* [1990].

[10] We also estimate the total RF due to BB by comparing the net radiation fluxes using aerosol and O_3 distributions from a MOZART simulation without BB aerosol

[1] Auxiliary material data sets are available at ftp://ftp.agu.org/apend/gl/2006gl028149. Other auxiliary material files are in the HTML.

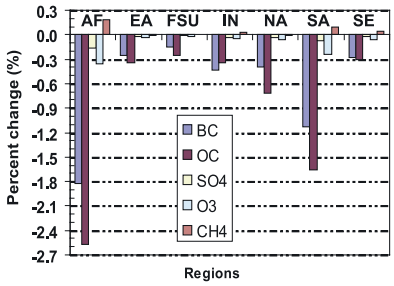

Figure 2. Percentage change in annual global mean burden of tropospheric O_3, steady state CH_4 and aerosols (OC, BC, $SO_4^=$) due to a 10% reduction in regional biomass burning emissions of short-lived O_3 precursors and aerosols relative to a base simulation. The change in tropospheric O_3 burden includes the contribution from a primary mode perturbation to CH_4.

and O_3 precursor emissions and with those using the base distributions (see auxiliary material). We calculate the global mean total sky RF due to BB aerosols and O_3 (including contributions from short-lived and primary mode) to be 0.13 Wm^{-2} and 0.11 Wm^{-2}, respectively. Our estimated positive BB aerosol RF is similar to the estimate of *Reddy et al.* [2005], but differs from previous estimates of negative BB aerosol RF [*Ramaswamy et al.*, 2001], suggesting the need for further investigations to verify the sign and magnitude of the net RF due to BB aerosols (see auxiliary material). We did not find any previous estimate of the RF due to O_3 produced exclusively from BB emissions in the literature (see auxiliary material).

3. Results and Discussion

[11] Although biomass burning emissions vary significantly with season, here we focus on the annual mean concentration changes of tropospheric O_3 and aerosols resulting from reduced BB emissions in each region. Regional reductions in BB emissions produce spatially inhomogeneous reductions in O_3 and aerosol concentrations, with largest decreases occurring near the region where BB was reduced (see auxiliary material). As Figure 2 shows, the largest decreases in global burdens of tropospheric O_3 and aerosols are simulated for 10% BB emission reductions in Africa (−0.36% O_3, −2.6% OC, −2.0% BC and −0.2% $SO_4^=$) and South America (−0.24% O_3, −1.7% OC, −1.1% BC and −0.1% $SO_4^=$), the regions with the largest BB sources. The smallest reduction in O_3 and aerosol burdens are simulated for emission reductions from the Former Soviet Union. The magnitude of reduction depends not only on the intensity of the emissions from each region but also on the regional chemistry and meteorology, particularly in the case of O_3. For example, simulated decreases in O_3 burdens for emission reductions from Southeast Asia and North America (Figure 2) are of similar magnitude although precursor emissions from Southeast Asia are half those from North America (Figure 1). Strong photochemical and convective activity increase the O_3 production efficiency (OPE) of NO_x from BB emissions in tropical regions (Southeast Asia, South America), consistent with the results of *Fuglestvedt et al.* [1999] and *Naik et al.* [2005] (Table 1). Because of relatively high levels of BB and the associated low VOC/NO_x emission ratios from savanna fires in Africa, the OPE for NO_x from Africa is lower than from Southeast Asia or South America.

[12] The reduction in short-lived O_3 precursors excites a primary mode perturbation that increases CH_4 for emission reductions from all regions except East Asia, the Former Soviet Union, and North America (Figure 2). These extratropical regions are characterized by forest fires that have high VOC/NO_x emission ratios [*Andreae and Merlet*, 2001]. Therefore, decreased CO and NMVOC emissions in these regions counteract the effect of decreased NO_x emissions causing a steady-state increase in OH and a decrease in CH_4.

[13] Among aerosol species, OC and BC are reduced significantly (up to −2.6% and −2.0% respectively, from Africa) as compared to $SO_4^=$ (up to −0.2% from Africa), as BB is only a minor source of SO_2 relative to fossil fuel combustion. The percent reduction in global burdens of OC and BC (Figure 2) is proportional to the contribution of regional BB to the global total emission of these species (Figure 1). Emission reductions from predominantly boreal and temperate forest burning regions (the Former Soviet Union and North America) result in a higher fraction of global OC versus BC reduced (∼1.8 times) compared with tropical forest and savanna burning. For regions dominated by agricultural waste burning the fraction of OC reduced is small (Southeast Asia ∼1.1) or even less than the fractional reduction in BC (India ∼0.8).

[14] Figure 3 (top) shows the change in global mean total-sky (includes cloudy and clear sky conditions) direct RF due to combined changes in aerosols, tropospheric O_3 (short-lived and primary mode) and CH_4 (from primary mode). BB emission reductions result in a negative O_3 radiative forcing, with amplitudes related to the reduced O_3 burdens. The largest negative O_3 forcing occurs for BB emission reductions from Africa followed by South America and the smallest for the Former Soviet Union. The CH_4 forcing is positive for all regions, except for East Asia, the Former Soviet Union, and North America, for which CH_4 concentrations decreased. The CH_4 RF is small compared to the O_3 RF, resulting in a net negative gas RF (from O_3 and CH_4 together) for all regions, implying a cooling tendency. These results confirm the conclusions of *Naik et al.* [2005] that combined reductions in anthropogenic NO_x, CO, and NMVOC emissions result in net negative radiative forcing from O_3 and CH_4.

[15] Because BC is an absorbing aerosol, a decrease in its burden results in a reduced radiative warming tendency (negative forcing), while a decrease in the burdens of

Table 1. O_3 Production Efficiency for Biomass Burning Calculated as the Ratio of the Change in Global Mean Tropospheric O_3 Burden to the Change in NO_x Emissions From Each Region

Region	O_3, Tg/TgN yr^{-1}
AF	2.70
EA	2.04
FSU	1.60
IN	2.42
NA	2.44
SA	3.77
SE	5.28

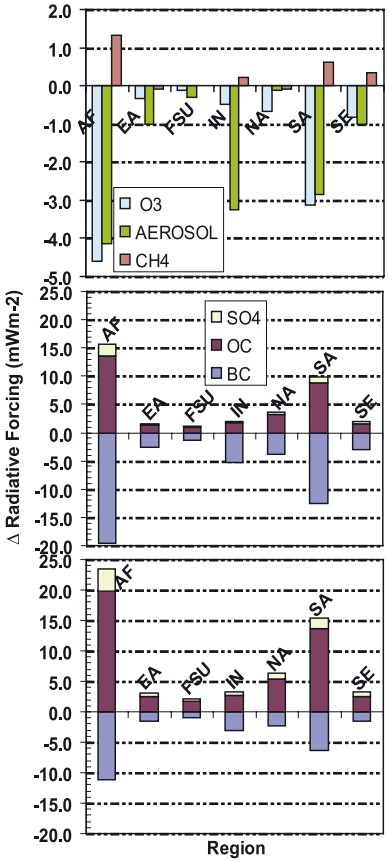

Figure 3. Change in total-sky global annual mean RF due to (top) O_3, CH_4 and aerosol (external mixture of carbonaceous aerosols and sulfates referred to as AEROSOLS), (middle) BC, OC and $SO_4^=$, and (bottom) change in clear sky RF due to BC, OC and $SO_4^=$ from a 10% reduction in regional biomass burning emissions of O_3 precursors and aerosols.

scattering aerosols, OC and $SO_4^=$, results in a reduced radiative cooling tendency (positive forcing). We calculate that the balance of absorbing and scattering aerosols produces a negative global annual mean total-sky direct RF for AEROSOL for all regions considered (Figure 3, top). The largest forcing amplitudes are simulated for emission reductions from tropical regions, including Africa, India and South America, and the smallest for emission reductions from extra-tropical regions, including North America and the Former Soviet Union. To evaluate the contribution of individual species to the total aerosol forcing, we consider the direct RF of each aerosol species separately. Figure 3 (middle) shows that negative RF from reduced BC burden is about 1.5 times the positive RF from the OC and $SO_4^=$ reductions, despite the larger OC burden reductions. One reason for the dominance of BC RF is that the forcing efficiency (ratio of radiative forcing to the change in burden) of BC is an order of magnitude greater than that of OC and $SO_4^=$ [*Menon*, 2004]. Besides optical properties, the vertical profile of BC and clouds play a significant role in determining the forcing efficiency of BC. Previous studies suggest that RF due to BC is enhanced if BC is above clouds but is lowered if the BC is below the clouds [*Haywood and Boucher*, 2000]. As shown in Figure 3 (bottom), in the absence of clouds the negative BC RF would be reduced, causing the positive RF from OC to dominate.

[16] To assess the sensitivity of RF changes to the location of biomass burning, we normalize the calculated gas and aerosol RF by the decrease of biomass burned in each region (Figure 4). We find that gas and aerosol RFs are most sensitive to BB in tropical regions with lower amounts of biomass burned (India, Southeast Asia, and East Asia). The gas and aerosol RF per unit biomass burned for India exceed those for Africa by factors of 2 and 18, respectively. The higher sensitivity of aerosol RF to the amount of biomass burned in India may be attributed to the higher fraction of radiatively efficient BC emitted from agricultural waste burning than from other types of BB. Meteorological conditions, including the presence of clouds, may also contribute to the higher sensitivity of aerosol RF from BB in India. We note the large uncertainties in estimates of the amount of biomass burned, particularly for agricultural waste burning [*Hao and Liu*, 1994; *Andreae and Merlet*, 2001] that need to be resolved to accurately assess the sensitivity of O_3 and aerosol forcing to the location of biomass burning.

4. Conclusions

[17] We have demonstrated that reductions in biomass burning (BB) emissions from major biomass burning regions of the world lead to a negative radiative forcing (cooling) from tropospheric O_3 and aerosols. The magnitude of this forcing depends strongly on the location of BB. Marginal reductions in BB emissions in tropical regions, including Africa, South America and India yield the largest negative radiative forcing. We find that global radiative forcing from aerosols and O_3 is most sensitive to changes in the amount of biomass burnt in India.

[18] Our results are a first step in determining changes in radiative forcing resulting from regional controls on BB. As illustrated by the wide range of BB aerosol RF values reported by model inter-comparison within the AeroCom initiative, the sign of RF due to BB aerosols is highly uncertain and much of this uncertainty arises from an inadequate representation of cloud properties, and the relative vertical position of aerosols and clouds [*Schulz et al.*, 2006]. Hence, the possibility of enhancing radiative warming tendency by reducing BB aerosols cannot be ruled out. Our results should, therefore, be used with caution and

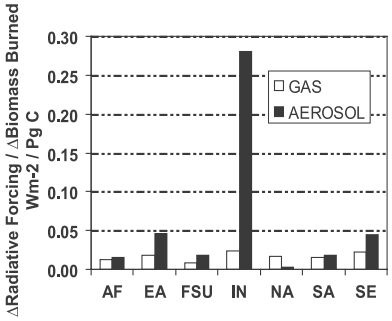

Figure 4. Normalized total sky gas (O_3 + CH_4) and aerosol radiative forcing per unit biomass burned in each region.

should be subject to further analysis and assessment. Uncertainties in the amount of biomass burned regionally, fire types, and emission factors will strongly impact our results. We have not considered the strong seasonal and interannual variability in BB driven by the availability of biomass, meteorological factors and human practices. We also have not included reductions of CH_4 emissions from BB, the direct RF from reduced CH_4 or the impact of reduced CH_4 emissions on O_3 and its radiative forcing. Including these factors would result in a larger negative radiative forcing from mitigating BB. Despite these limitations, we have demonstrated significant regional differences in the net radiative impact of biomass burning. These regional variabilities need to be considered when evaluating controls on biomass burning to mitigate global climate change.

[19] **Acknowledgments.** V. Naik was supported by the Carbon Mitigation Initiative (CMI) of the Princeton Environmental Institute at Princeton University (www.princeton.edu/∼cmi) which is sponsored by BP and Ford. We thank Paul Ginoux for helpful discussions and Jason West for valuable comments on an earlier version of this manuscript. We are grateful to two anonymous reviewers for providing helpful comments on the submitted manuscript.

References

Andreae, M. O. (1991), Biomass burning: Its history, use, and distribution and its impact on environmental quality and global climate, in *Global Biomass Burning: Atmospheric, Climatic, and Biospheric Implications*, edited by J. S. Levine, pp. 3–21, MIT Press, Cambridge, Mass.

Andreae, M. O., and P. Merlet (2001), Emission of trace gases and aerosols from biomass burning, *Global Biogeochem. Cycles*, *15*, 955–966.

Committee on Radiative Forcing Effects on Climate (2005), *Radiative Forcing of Climate Change: Expanding the Concept and Addressing Uncertainties*, Natl. Acad. Press, Washington, D. C.

Fuglestvedt, J. S., et al. (1999), Climatic forcing of nitrogen oxides through the changes in tropospheric ozone and methane: Global 3D model studies, *Atmos. Environ.*, *33*, 961–977.

GFDL Global Atmospheric Model Development Team (2004), The new GFDL global atmosphere and land model AM2-LM2: Evaluation with prescribed SST simulations, *J. Clim.*, *17*, 4641–4673.

Ginoux, P., L. W. Horowitz, V. Ramaswamy, I. V. Geogdzhayev, B. N. Holben, G. Stenchikov, and X. Tie (2006), Evaluation of aerosol distribution and optical depth in the Geophysical Fluid Dynamics Laboratory coupled model CM2.1 for present climate, *J. Geophys. Res.*, *111*, D22210, doi:10.1029/2005JD006707.

Hao, W. M., and M. H. Liu (1994), Spatial and temporal distribution of tropical biomass burning, *Global Biogeochem. Cycles*, *8*, 495–503.

Haywood, J., and O. Boucher (2000), Estimates of the direct and indirect radiative forcing due to tropospheric aerosols: A review, *Rev. Geophys.*, *38*, 513–543.

Horowitz, L. W., et al. (2003), A global simulation of tropospheric ozone and related tracers: Description and evaluation of MOZART, version 2, *J. Geophys. Res.*, *108*(D24), 4784, doi:10.1029/2002JD002853.

Intergovernmental Panel on Climate Change (1990), *Climate Change 1990: The Intergovernmental Panel on Climate Change Scientific Assessment*, edited by J. T. Houghton et al., Cambridge Univ. Press, New York.

Jacobson, M. Z. (2004), The short-term cooling but long-term global warming due to biomass burning, *J. Clim.*, *17*, 2909–2926.

Kiehl, J. T., et al. (1998), The National Center for Atmospheric Research Community Climate Model: CCM3, *J. Clim.*, *11*, 1131–1149.

Kim, J. H., and M. J. Newchurch (1996), Climatology and trends of tropospheric ozone over the eastern Pacific Ocean: The influences of biomass burning and tropospheric dynamics, *Geophys. Res. Lett.*, *23*, 3723–3726.

Mauzerall, D. L., J. A. Logan, D. J. Jacob, B. E. Anderson, D. R. Blake, J. D. Bradshaw, B. Heikes, G. W. Sachse, H. Singh, and B. Talbot (1998), Photochemistry in biomass burning plumes and implications for tropospheric ozone over the tropical South Atlantic, *J. Geophys. Res.*, *103*, 8401–8423.

McKeen, S. A., G. Wotawa, D. D. Parrish, J. S. Holloway, M. P. Buhr, G. Hübler, F. C. Fehsenfeld, and J. F. Meagher (2002), Ozone production from Canadian wildfires during June and July of 1995, *J. Geophys. Res.*, *107*(D14), 4192, doi:10.1029/2001JD000697.

Menon, S. (2004), Current uncertainties in assessing aerosol effects on climate, *Annu. Rev. Environ. Resour.*, *29*, 1–30.

Ming, Y., V. Ramaswamy, P. A. Ginoux, and L. H. Horowitz (2005), Direct radiative forcing of anthropogenic organic aerosol, *J. Geophys. Res.*, *110*, D20208, doi:10.1029/2004JD005573.

Müller, J.-F. (1992), Geographical distribution and seasonal variation of surface emissions and deposition velocities of atmospheric trace gases, *J. Geophys. Res.*, *97*, 3787–3804.

Naik, V., D. Mauzerall, L. Horowitz, M. D. Schwarzkopf, V. Ramaswamy, and M. Oppenheimer (2005), Net radiative forcing due to changes in regional emissions of tropospheric ozone precursors, *J. Geophys. Res.*, *110*, D24306, doi:10.1029/2005JD005908.

Ramaswamy, V., et al. (2001), Radiative forcing of climate change, in *Climate Change 2001: The Scientific Basis*, edited by J. T. Houghton et al., pp. 349–416, Cambridge Univ. Press, New York.

Reddy, M. S., O. Boucher, Y. Balkanski, and M. Schulz (2005), Aerosol optical depths and direct radiative perturbations by species and source type, *Geophys. Res. Lett.*, *32*, L12803, doi:10.1029/2004GL021743.

Schulz, M., et al. (2006), Radiative forcing by aerosols as derived from the AeroCom present-day and pre-industrial simulations, *Atmos. Chem. Phys.*, *6*, 5225–5246.

Streets, D. G., K. F. Yarber, J.-H. Woo, and G. R. Carmichael (2003), Biomass burning in Asia: Annual and seasonal estimates and atmospheric emissions, *Global Biogeochem. Cycles*, *17*(4), 1099, doi:10.1029/2003GB002040.

Streets, D. G., T. C. Bond, T. Lee, and C. Jang (2004), On the future of carbonaceous aerosol emissions, *J. Geophys. Res.*, *109*, D24212, doi:10.1029/2004JD004902.

Thompson, A. M., et al. (2001), Tropical tropospheric ozone and biomass burning, *Science*, *291*, 2128–2132.

Textor, C., et al. (2006), Analysis and quantification of the diversities of aerosol life cycles with AeroCom, *Atmos. Chem. Phys.*, *6*, 1777–1813.

Tie, X., S. Madronich, S. Walters, D. P. Edwards, P. Ginoux, N. Mahowald, R. Zhang, C. Lou, and G. Brasseur (2005), Assessment of the global impact of aerosols on tropospheric oxidants, *J. Geophys. Res.*, *110*, D03204, doi:10.1029/2004JD005359.

Wild, O., M. J. Prather, and H. Akimoto (2001), Indirect long-term global cooling from NO_x emissions, *Geophys. Res. Lett.*, *28*, 1719–1722.

L. W. Horowitz, V. Ramaswamy, and M. D. Schwarzkopf, Geophysical Fluid Dynamics Laboratory, NOAA, Princeton, NJ 08540, USA.

D. L. Mauzerall, V. Naik, and M. Oppenheimer, Woodrow Wilson School of Public and International Affairs, Princeton University, Robertson Hall 403, Princeton, NJ 08544, USA. (vnaik@princeton.edu)